Conference title

Testing ZnO based photoanodes for PEC applications

Mareike Trunk[a,*], Agnieszka Gorzkowska-Sobas[b], Vishnukanthan Venkatachalapathy[a], Tianchong Zhang[a], Augustinas Galeckas[a], Andrej Yu. Kuznetsov[a]

Department of Physics/Centre for Materials Science and Nanotechnology, University of Oslo, P.O. Box 1126 Blindern, N-0318 Oslo, Norway
Department of Chemistry/Centre for Materials Science and Nanotechnology, University of Oslo, P.O. Box 1126 Blindern, N-0318 Oslo, Norway

Abstract

We report on multi layered ZnCdO photoanode structures synthesized on c-Al_2O_3 substrates using metal organic vapor phase epitaxy and covered with a thin TiO_2 protective film using atomic layer deposition and pulsed laser deposition techniques. Structural, optical and photoelectrochemical properties of the multilayers were investigated systematically in connection with their potential application in the photolysis of water. X-ray diffraction and Rutherford backscattering techniques confirmed staggered arrangement and graded Cd content of the multilayers. Temperature-dependant photoluminescence revealed excitonic nature of a broad emission band representing combined band-edge emissions from the individual layers. The photocurrent was found to increase with decreasing thickness of the TiO_2 protective layer.

Keywords: ZnCdO; photoanode; photocorrosion; photoluminescence.

1. Introduction

The continual need of suitable semiconducting materials in the fields of optoelectronics and photovoltaics has raised the interest in ZnO-based alloys. A crucial step towards practical device implementation depends on the mastering of the band gap engineering, which allows for more efficient absorption of the solar spectrum. Besides applications in solar cells [1] and lighting technology [2], ZnO has been discussed as a photoanode in photoelectrochemical (PEC) cell [3,4] for water splitting. Ever since 1972, when Fujishima and Honda [5] demonstrated water splitting via photolysis utilizing TiO_2 as a photoanode, metal oxides - and among those ZnO - have gained a lot of interest in this field [6,7]. However, for a semiconductor in the role of a photoelectrode, certain requirements have to be fulfilled in terms of band gap, band edge positions and chemical stability [8]. Since combining both matching band gap and chemical stability in one material is very challenging, attempts have been made to delegate these two functions in the cell to different materials [9,10]. Indeed, the valence and conduction band edges of ZnO straddle the redox levels of water, thus rendering spontaneous photoelectrolysis possible, and by mixing ZnO with CdO the band gap can be readily tuned from ~ 3.4 eV (ZnO) to 2.3 eV (CdO), allowing for light absorption in the desired spectral region. At the same time, ZnO dissolves in most electrolytes [11] making an anticorrosion layer indispensable. Among other oxides, TiO_2 is know to be chemically stable, making it a potential

candidate for a thin photoanode overlayer preventing corrosion of the underlying electrode [5,12]. The efficiency of PEC cells may be further increased by stacking several layers of ZnCdO with a variable Cd content into a multilayer (ML) structure, which will readily cover a wider range of the solar spectrum. In addition, a gradient of the electrical field created across the sample could be beneficial for fast carrier transfer trough the structure. A similar principle is applied in multi-junction solar cells where multiple layers of semiconductors with different band gaps are used to harvest light from a wider range of the solar spectrum. However, the synthesis of single phase ZnCdO alloys in a broad range of Cd content is a nontrivial issue due to the different crystal structures of ZnO and CdO; ZnO crystallizes in wurtzite and CdO in rock-salt structure. Indeed, possible coexistence of multiple phases as well as polycrystalline structure has been reported for as-grown ZnCdO alloys [13,14]. In this article, we report on the preparation of ZnCdO ML structures by metalorganic vapor phase epitaxy (MOVPE) and on structural and optical characterization of the films including transmittance, diffuse reflectance and low temperature photoluminescence measurements. Finally, we discuss the PEC performance of ZnCdO-TiO_2 photoanode structures in terms of the Cd content and the protective TiO_2 overlayer.
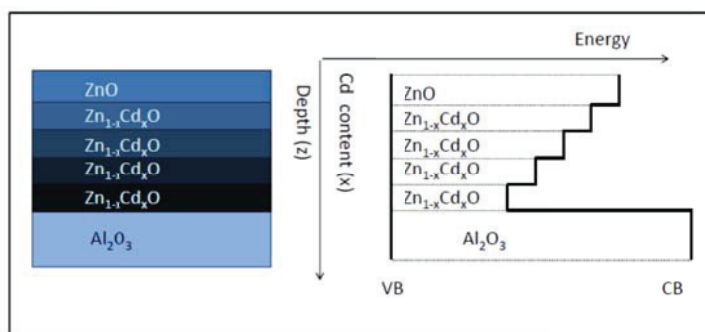

Fig. 1. Schematics of the composition and electronic structure of the investigated ZnCdO multilayers .

2. Experimental

2.1 Sample preparation

The investigated ZnO based photoelectrodes were synthesized on c-Al_2O_3 by MOVPE using a commercial reactor (TITAN/EMF) keeping the chamber temperature at 370 °C and the chamber pressure at 600 mbar. Diethyl zinc (DEZn), Dimethyl cadmium (DMCd), and tertiary butanol (t-BuOH) were used as zinc, cadmium and oxygen sources, respectively. Figure 1 shows a schematics of such a ZnCdO multilayer structure, which is comprised of five different $Zn_{1-x}Cd_xO$ alloy layers. The thickness of individual layers was varied in the range of $10 - 50$ nm, but being constant for all five single layers within each ML structure. Upon film deposition, selected samples were annealed at 800 °C in oxygen atmosphere for 3 and 10 min, respectively. The TiO_2 protective films were deposited using both pulsed layer deposition (PLD) and atomic layer deposition (ALD) techniques yielding a thickness between 5 and 50 nm. Then a part of the TiO_2 film and underlying Zn(Cd)O material was removed by laser ablation to provide a reliable electrical contact to the bottom ZnCdO layer (in Fig. 1).

2.2 Structural and optical analysis

Optical absorption properties of ML structures were derived from the transmittance and diffuse reflectance measurements performed at room temperature using UV-VIS spectrophotometer (ThermoScientific EVO-600). Photoluminescence (PL) was investigated in the temperature range from 10 K to 300 K by employing 325 nm wavelength of cw He-Cd laser with an output power of 10mW as an excitation source. The emission was collected

by a microscope and directed to fiber optic spectrometer (Ocean Optics USB4000, spectral resolution 2 nm). Temperature dependent measurements were performed using a closed-cycle He-refrigerator (Janis, Inc. CCS450). The chemical composition of the samples was measured by Rutherford backscattering spectrometry (RBS), while the crystalline structure of the films was analyzed by X-ray diffraction (XRD). More details on growth and characterization of ZnCdO alloys with variable Cd content can be found elsewhere [13]. The surface observations were carried out using a scanning electron microscope (SEM) FEI Quanta 200 FEG-ESEM equipped with EDAX-EDS.

2.3 *PEC measurements*

PEC behavior of the ZnCdO photoanodes was investigated by voltammetric measurements in a 3-electrode cell, where Pt wire was used as a reference electrode and a saturated calomel electrode (SCE, Sigma-Aldrich) as a reference electrode. Linear Sweep Voltammetry (LSV) was measured by a Parstat 2267 potentiostat/galvanostat in a range of -0.5 to 1.5 V vs. SCE. Sodium sulfate water solution with molar concentrations of 1 mol/dm^3 was used as electrolyte. The photocurrent was recorded under AM1.5 and AM0 illumination using a solar simulator (Oriel). Additionally, short circuit current was recorded under the same illumination conditions as a function of time. The solutions were purged with N_2 prior to measurements. The required ohmic contacts on the back of the samples were made using silver paste and Cu tape.

3. Results and Discussion

3.1 *Structural characterization*

The SEM image presenting typical morphological features of the ML structure is shown in Fig. 2a. The film is fairly crystalline and consists of the grains of approx. 100 nm size. The ML surface after TiO_2 protective film deposition is presented in Fig. 2b. The TiO_2 deposition is followed by only minor changes in the microstructure of the surface. The surface features become smoother, yet the shape and grain size is preserved which may indicate that the TiO_2 film covers the ML uniformly and the TiO_2 overlayer reflects the underlaying morphological features. This is in agreement with the XRD results revealing amorphous nature of the TiO_2 films. The film seems to be continuous, however, we cannot exclude the presence of nanometer size pinholes, considering the results of the electrochemical measurements (see below). Figure 2c shows the image taken at the spot that was exposed to electrochemical measurements. After the electrochemical measurement, a slight decoloration of the film occurred, which is reflected by the change in surface morphology. As can be seen the surface features become coarser and the image resembles the surface before TiO_2 deposition. This possibly denotes that the TiO_2 protective layer is no longer present on the ML surface, which is also confirmed by EDS results.
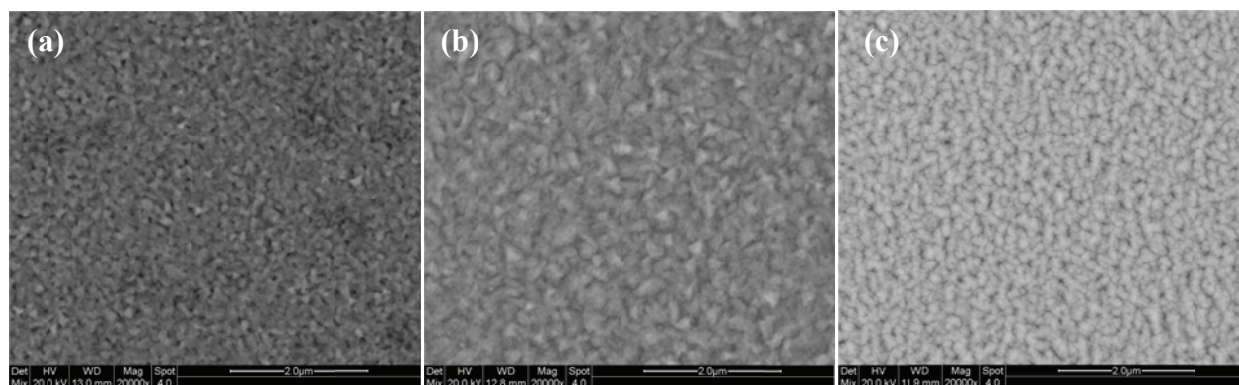

Fig. 2. SEM pictures showing a ZnCdO ML layer structure (a) before TiO_2 deposition, (b) after TiO_2 deposition and (c) after electrochemical measurements.
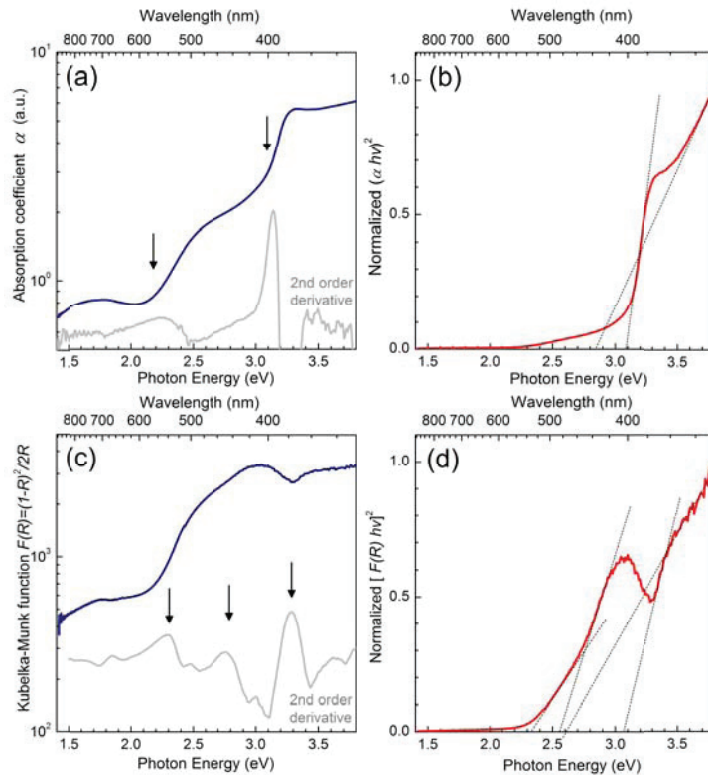
Fig. 3. Absorption edge of the ZnCdO ML structure (ML250_10'annealed) deduced from transmittance (a) and diffuse-reflectance (c) measurements at 300 K; arrows indicate apparent absorption sub-thresholds; (b, d) are corresponding Tauc plots considering direct optical transitions in ZnCdO multilayer structures.

3.2 *Optical characterization*

Optical absorption properties of the ML structures were investigated at room temperature by means of UV-Visible transmittance and diffuse-reflectance spectroscopy (DRS). The band gap energies and the dominant type of optical transitions were determined using standard Kubelka-Munk [15] and Tauc [16] treatment of the spectra. The absorption edge deduced from the transmittance and DRS of sample ML250nm_10'annealed (i.e. ZnCdO ML structure with a thickness of 250 nm and a post growth annealing time of 10 min) and are summarized in Fig. 3, where several prominent absorption sub-thresholds associated with different layers are indicated by arrows. Normalized Tauc plots presented in Figs. 3b and 3d suggest involvement of predominantly direct optical transitions in the absorption process.

Low-temperature photoluminescence measurements were performed to get a better insight into the role of individual layers. Figure 4 summarizes the photoluminescence spectra taken at 10 K for ML structures having (i) different thickness of the individual layers and (ii) post-growth annealing time. For comparison, a spectrum of pure ZnO single layer film is shown as well. The near-band-edge (NBE) transitions in pure ZnO material are known to peak at around 3.4 eV and exhibit gradual red-shift down to 2.3 eV upon alloying with Cd [17]. As one can see, typical PL spectra of ML are characterized by a broad band stretching in the range from 3.3 to 2.5 eV, which are composed of several NBE emissions from the individual layers, as indicated by arrows in Fig. 4b. Temperature dependent PL measurements (see Fig. 4b and 4c) revealed excitonic nature of all single peaks forming the plateau, thus proving optical activity of all constituents of the ML structure in the processes of absorption and emission. Similar excitonic transitions could also be observed in the other ML samples. In the present article,

ML250nm_10'annealed was chosen for further PEC testing as a promising candidate showing optical response in the range of interest for water splitting. In the following, this sample will be referred to as ZnCdO ML structure.
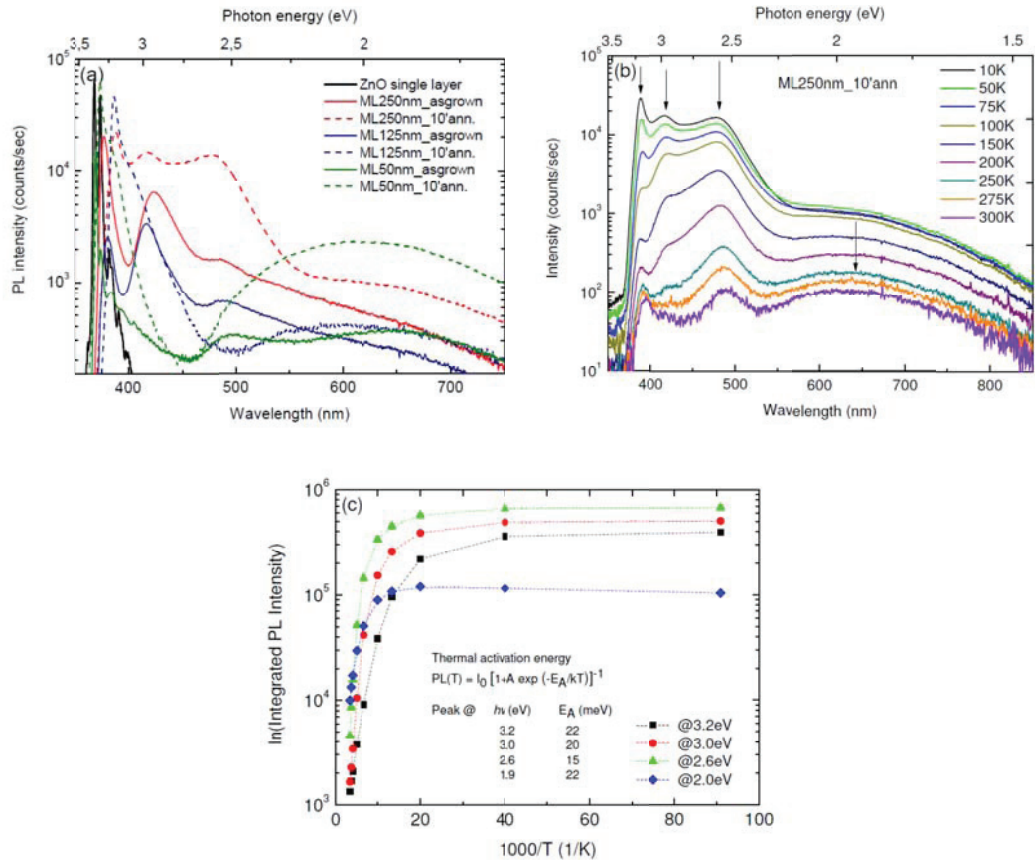

Fig. 4: Typical PL spectra recorded at 10K of ZnCdO ML having different thicknesses and post growth annealing times (panel a) and characteristic temperature dependence of the PL intensity (b) with the corresponding Arrhenius plot shown in (c).
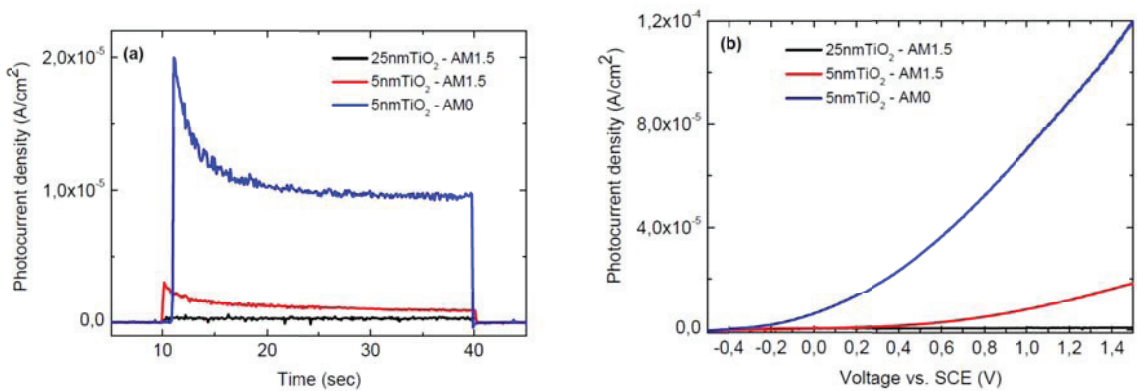

Fig. 5 The graph presents (a) the kinetic behavior and (b) J-V curves for ZnCdO ML electrodes with 5 nm and 25 nm thick TiO₂ protective films measured under AM1.5 and AM0.

3.3 *Photoelectrochemical characterization*

Figure 5a and b show the results of the photocurrent response measurements performed under AM 1.5 and AM0 illumination, without external bias applied. With no illumination, only residual current of a few nanoamps is observed. Exposure to light yields a photoanodic spike and after a while the photocurrent decreases reaching saturation level. The source of the anodic spike might be due to crystal defects as suggested by Radecka et al. [18]. There, a fast decay in the photoanodic spike indicates the increased recombination process and was attributed to the point defects resulting from incorporation of foreign atoms. This in turn leads to an increase in the number of the recombination sites. In our case, we believe that for the ML structure the greatest contribution to the recombination centers in the film can be attributed to the presence of the multiple interfaces. In addition, it was also shown that the presence of Cd leads to worsening of the film crystallinity due to the ionic radius mismatch.

As can be seen the increase in TiO_2 protective layer thickness is followed by a significant decrease in the photocurrent intensity. This may indicate that the observed high values for the 5 nm TiO_2 protective film are due to corrosion processes occurring on the sample surface exposed to the electrolyte. This observation is supported by the fact the J-V curves presented in Fig. 4b do not show a saturation current. Post mortem observations revealed a discoloration of the samples after the PEC testing in the area exposed to the solution (see section 3.1). TiO_2 is highly resistive towards electrochemical and photochemical corrosion and it was previously shown that thin films are sufficient to prevent the electrolyte from diffusing through the protective layer [19]. However any discontinuities in the film created either during the deposition or the handling will lead to the penetration of the electrolyte through the pinholes and the subsequent reaction with the Zn ions from the lattice according to the reaction: $ZnO + 2H^+ \rightarrow Zn^{2+} + H_2O$ [20]. Once the contact between the TiO_2 protective layer and the ML is broken, the TiO_2 no longer adheres to ML and peels off easily, exposing the ML to the further electrochemical corrosion, as it can be seen from SEM observations.

A change in the illumination conditions is followed by a 10-folded increase in the photocurrent response of the ML. Indeed, the light utilized under AM0 has an enhanced UV part which coincides with the ZnO fundamental absorption edge. Thus, we suggest that the observed photoresponse is dominated by the ZnO film on top of the ML structure, while carriers photoexcited in the deeper films buried under ZnO layer may be stopped at interfaces between the single films.

4. Conclusion

The systematic study of ZnCdO ML structures has lead to the conclusion that optical emission band is broadened for ML ZnCdO structures compared to single film ZnO which can be explained by combined band-edge emissions from the individual layers. In addition, temperature-dependant studies reveal excitonic nature of all individual layers in the ML structure. In case of the PEC measurements the highest photocurrent intensity was observed for the UV-rich illumination, which may be attributed to the dominating role of the pure ZnO layer in the ML photoanodic device. However, there is a need to improve the TiO2 protective layers, since the applied films proved to be insufficient in preventing efficiently the ML from corrosion processes occurring under the measurement conditions.

Acknowledgements

References

1. D.G. Baik and S.M. Cho, Thin Solid Films 345 (1999) 227.
2. C. Bayram, F.H. Teherani, D.J. Rogers,and M. Razeghi, Applied Physics Letters 93 (2008) 081111.
3. A. Wolcott, W.A Smith, T.R Kuykendall, Y.P. Zhao, and J.Z. Zhang, Advanced Functional Materials 19 (2009) 1849.

4. M.Gupta, V. Sharma, J. Shrivastava, A. Solanki, A.P. Singh, V.R. Satsangi, S. Dass, and R. Shrivastav, Bulletin of Materials 32 (2009) 23.

5. A. Fujishima and K. Honda, Nature 238 (1972) 37.

6. B.D Alexander, P.J. Kulesza, L. Rutkowska, R. Solarska, and J. Augustynski, Journal of Materials Chemistry 18 (2008) 2298.

7. V.M. Aroutiounian, V.M. Arakelyan, and G.E. Shahnazaryan, Solar Energy 78 (2005) 581.

8. T. Bak, J. Nowotny, M. Rekas, and C.C. Sorrell, International Journal of Hydrogen Energy 27 (2002) 991.

9. W. Siripala, A. Ivanovskaya, T.F. Jaramillo, S.H. Baeck, and E.W. McFarland, Solar Energy Materials and Solar Cells 77 (2003) 229.

10. Y. Bessekhouad, D. Robert, and J. Weber, Journal of Photochemistry and Photobiology A- Chemistry 163 (2004) 569.

11. G.H. Schoenmakers, D. Vanmaekelbergh, and J.J. Kelly, Journal of the Chemical Society – Faraday Transactions 93 (1997) 1127.

12. H. Morisaki, T. Watanabe, M. Iwase, and K. Yazawa, Applied Physics Letters 29 (1976) 338.

13. V. Venkatachalapathy, A. Galeckas, M. Trunk, T. Zhang, A. Azarov, and A. Yu. Kuznetsov, Physical Review B 83 (2011) 125315

14. C.X. Shan, Z. Liu, Z.Z. Zhang, D.Z. Shen, and S.K. Hark, Journal of Physical Chemistry B 110 (2006) 11176.

15. P. Kubelka and F.Z. Munk, Technical Physics 12 (1931) 593.

16. J. Tauc, R. Grigorovici, and A. Vancu, Physica Status Solidi 15 (1966) 627.

17. T. Gruber, C. Kirchner, R. Kling, F. Reuss, A. Waag, F. Bertram, D. Forster, J. Christen, and M. Schreck, Applied Physics Letters 83 (2003) 3290.

18. M. Radecka, M. Rekas, A. Trenczek-Zajac, and K. Zakrzewska, Journal of Power Sources 181 (2008) 46.

19. C.X. Shan, X.H. Hou, and K.L. Choy, Surface & Coatings Technology 202 (2008) 2399.

20. L.W. Zhang, H.Y. Cheng, R.L. Zong, and Y.F. Zhu, Journal of Physical Chemistry C 113 (2009) 2368.